Proceedings of The National Conference
On Undergraduate Research (NCUR) 2016
University of North Carolina Asheville
Asheville, North Carolina
April 7-9, 2016

"Effect of High Surface Area Carbon Addition on the Performance of a Non-Precious Metal Catalyst in a PEM Fuel Cell"

Christopher A. Neal
Department of Chemical and Biomolecular Engineering
The University of Tennessee at Knoxville
Knoxville, TN 37996

Faculty Advisors: [1]Nelly Cantillo, [2]Shengqian Ma, [1]Gabriel A. Goenaga and [1,3]Thomas A. Zawodzinski

[1]Department of Chemical and Biomolecular Engineering
The University of Tennessee at Knoxville
Knoxville, TN 37996

[2]Department of Chemistry
The University of South Florida
Tampa, FL 33620

[3]Physical Chemistry of Materials Group
Oak Ridge National Laboratory
Oak Ridge, TN 37831

Abstract

In Polymer Electrolyte Membrane Fuel Cells (PEMFCs), the structure and morphology of the electrode layer directly affect the value of the electrochemical resistance, which has an impact on the cell performance. The effects of these parameters become particularly significant when the cathode catalyst is based on a non-precious metal due to the higher catalyst loadings required to compensate for the lower catalytic activity when compared to Pt based catalysts. In previous experiments performed in our laboratory, a pyrolyzed iron (III) porphyrin framework (PCPF-Fe) material was characterized, exhibiting a good single cell performance. In this study, the addition of a high surface carbon to the PCPF-Fe was conducted in an attempt to increase the surface area and the electron conductivity and, consequently, improve the activity and stability of the material. For this purpose, as-synthetized PCPF-Fe was mixed with Ketjenblack® (KJB) carbon at four different ratios, pyrolyzed and its catalytic activity towards the oxygen reduction reaction (ORR) was evaluated using rotating ring disk electrode (RRDE) experiments. The structure and morphology of the catalyst layer were analyzed through scanning electron microscopy (SEM), and X-ray diffraction (XRD). The best performing mixture was 50% PCPF-Fe, and exhibited a higher onset potential (0.868 V in the 100% vs. 1.016 V in the 50%) and limiting current density (-4.6mA/cm^2 in the 100% vs. -6.0mA/cm^2 in the 50%) to that of the pure material. The material was then used as the cathode electrode in a single cell. The maximum current density obtained in single cell test for the 50% PCPF-Fe was only a third of that obtained with a 100% PCPF-Fe (0.25A/cm^2 vs. 0.81A/cm^2) cathode with the same catalyst loading, which could be a result of the lower density of catalytic centers in the mixture.

Keywords: Proton Exchange Membrane Fuel Cell, non- precious metal catalyst, catalysis

1. Introduction

As the world becomes increasingly aware of the dangers of global climate change, the need for "green" energy generation and storage becomes urgent. Additionally, some portable electronics require constant power sources that do not require repeated charging, as common alternatives such as lithium-ion and zinc-air batteries currently necessitate. Proton Exchange Membrane Fuel Cells (PEMFCs) have been proposed as a clean, portable power source, but current technological difficulties restrict their widespread implementation. The oxygen reduction reaction (ORR) that occurs at the cathode of the fuel cell is slow and requires a large amount of catalyst, greatly increasing the cost of the cell when using conventional platinum catalysts. This factor has encouraged the development of non-precious metal catalysts (NPMCs) that could decrease the cost of and increase the production of PEMFCs.

Common NPMC alternatives include catalysts derived from copper, cobalt, or iron heat-treated with nitrogen and carbon sources. This approach allows for countless combinations and ratios of metal/ nitrogen/ carbon, as well as numerous synthesis conditions. This method was introduced by Yeager et al. (1989), who studied the loading of poly(acrylonitrile) (PAN) and a metal precursor onto a carbon support, which was then pyrolyzed under argon gas at 800°C. The pyrolysis products exhibited fair ORR activity, comparable to that of heat-treated cobalt porphyrins.

Further work has shown that materials derived from heterocyclic polymers that contain both nitrogen and iron exhibit high potential for ORR catalysis. Lalande et al. (1997) discovered the individual importance of metals and nitrogen in the active site of catalysts through their work with polyvinylferrocene adsorbed on carbon black. Performance durability for polyamine-derived catalysts was explored by Zelenay (2009), who compared PANI and polypyrrole (PPy) as nitrogen precursors and found better selectivity and stability in PANI-derived materials. Attempts to decrease mass transport losses were made by Liu et al. (2010) who implemented a "uniformly decorated catalytic framework" to maximize micropore volume and active catalyst density. Proietti (2011) combined a zeolitic-imidazolate-framework and ferrous acetate to develop a catalyst precursor that demonstrated a respectable power density at 0.6 V (0.75 W cm^{-2}) by further decreasing mass transport losses.

Additionally, contributions by Cantillo (2016) have displayed a relatively high surface area and pore volume in the material PCPF-Fe, a covalent heme framework catalyst produced by Ma (2014). Unfortunately, both characteristics of the material decreased dramatically upon pyrolysis and heat treatment, limiting the power density of the material at a loading of $2mg_{cat}/\ cm^2$ to a still impressive 0.46 W/cm^2 in H_2-O_2 fuel cell testing for the ORR reaction. Cantillo noticed that when the "mass transport losses were 'artificially' reduced," a significant improvement in the ORR activity of the PCPF-Fe material occurred. Therefore, she theorized that realistically decreasing the mass transport losses of the material could in turn produce an increase in cell performance of the material.

In the present study, we analyzed the ORR activity of the PCPF-Fe catalyst combined with various amounts of a graphitic carbon source, Ketjenblack® (KJB). Theoretically, it was believed that addition of a high surface area carbon would increase the pore volumes, allowing for better access to active sites; this in turn would lower the resistance of the material from mass transport losses. Pyrolysis at 700ºC under inert atmosphere resulted in the ORR catalyst. The onset potential and number of electrons transferred by the catalyst were determined by rotating ring disk electrode experiments. The heat treated catalysts that showed the best performance in the rotating ring disk electrode experiment (RRDE) underwent a sulfuric acid treatment and additional heat treatment at 700 °C; these new samples were also tested in the RRDE. Characterization of the structure and properties of the materials were obtained using SEM, XRD, and energy-dispersive X-ray spectroscopy (EDS).

2. Methodology and Results

2.1 Catalyst Synthesis And Activation

The PCPF-Fe was prepared by adding iron (III) tetra (4-bromophenyl)porphyrin chloride to a solution of 2,2'bipyridyl, bis (1,5-cyclooctadiene)-nickel(0) and 1,5-cyclooctadiene in anhydrous DMF/1,4-dioxide. The mixture was then stirred under an inert atmosphere of argon overnight at room temperature, before being cooled in an ice bath. 50% acetic acid was then added and the mixture was again stirred overnight. Finally, the mixture was washed and dried with a vacuum to obtain a 78% yield of PCPF-Fe.

In order to increase the surface area, and the limiting current density, various amounts of KJB, an electroconductive carbon black, were added to samples of the as-synthesized PCPF-Fe. Starting with the 100 wt. % PCPF-Fe (control), samples of 50 wt. %, 43 wt. %, 33 wt. %, and 20 wt. % PCPF-Fe on KJB were produced. Because the control showed

very poor ORR catalytic activity as-synthesized, the samples were then pyrolyzed at 700°C under N_2 atmosphere for 1 h; this pyrolysis was what created the ORR active sites.

Samples that showed the best performance in rotating ring disk electrode experiments were then treated in 0.5 M H_2SO_4 at 80°C for 8 h to remove excess metals generated during pyrolysis. During high temperature treatment in the presence of carbon, iron can reduce to metallic iron, which can form nanoparticles; these particles can then block pores to active sites, thus lowering the maximum possible activity. Those samples were then pyrolyzed a second time at 700°C under a N_2 atmosphere for 1 h to promote further catalytic center formation.

2.2 Physicochemical Characterization

XRD, SEM, and EDS were implemented to characterize the materials. XRD patterns were measured with a Bruker D2 Phaser diffractometer with Cu Kα radiation. A Hitachi S-4800 field emission scanning electron microscope was employed for SEM imaging which features a 1.0 nanometer resolution and variable acceleration voltages ranging from 0.5kV to 30kV.

2.3 Rotating Ring Disk Electrode (RRDE) Experiments

Inks were produced by mixing 5 mg of the catalyst with 5 wt. % Nafion® solution (Sigma-Aldrich) at a 30:70 ionomer:catalyst ratio; methanol was then added as a solvent. Using a magnetic stir bar, the inks were allowed to stir for 24 h and then sonicated for 10 min before first use. Electrodes were prepared by depositing approximately 15 µL of the solution until a loading of 600 $\mu g/cm^2$ was achieved upon drying. A three-electrode cell system with Hg/Hg_2SO_4 reference electrode saturated with 0.5 M H_2SO_4 and a gold wire counter electrode were used. The reference electrode potential was measured against the reversible hydrogen electrode (RHE) by bubbling hydrogen gas through the electrolyte for 30 min; the open circuit potential was then measured using a Pt working electrode. The potential was observed to be 0.696 V vs. RHE. All further potentials reported are vs. RHE.

The working electrode contained a glassy carbon disk surrounded by a concentric platinum ring (AFE7R9GCPT from Pine Instruments) with a collection efficiency of 37%. A multi-channel VSP3 BioLogic Science Instruments potentiostat was used to control the electrode potential. The working electrode was constantly rotated at 1600 rpm using an AFMSRCE Pine Modulated Speed Rotator (MSR). Cyclic voltammograms were collected in a 0.1 M H_2SO_4 solution at room temperature at 10 mV/s scan rate with both static and rotating working electrodes. Voltammograms were first collected in the electrolyte solution saturated with nitrogen gas, for background correction, and then with oxygen. Before and after use, the glassy carbon disk was hand- polished with 5 µm and 0.05 µm alumina powder.

2.4 Membrane Electrode Assembly Preparation

Electrodes' preparation for fuel cell testing began by mixing 15 mg of the pyrolyzed catalyst sample with a 5 wt. % Nafion® solution in a 30 wt. % Nafion®/ 70 wt. % catalyst ratio. The ink was the dissolved in 1 g of deionized water and 2 g of isopropanol. The ink was sprayed onto a carbon gas diffusion layer (GDL, Sigracet® Gas Diffusion Media, Type GDL 25 BC) cut to an area of 5 cm^2 using an airbrush. Ink was sprayed onto the GDL until the desired loading (2 mg_{cat}/cm^2) was achieved. The thickness of the cathode was measured before and after catalyst- deposition using an Absolute Mitutoyo® Digimatic Indicator (Model ID-S112PE). The anode electrodes were prepared by airbrushing an ink onto a similar GDL to a loading of 0.2 mg_{cat}/cm^2. This ink was prepared from BASF 30% platinum on Vulcan® XC-72 with Nafion® in a 2 ionomer: 1 Pt ratio. The electrodes were then hot-pressed on either side of a Nafion® 212 membrane for 10 min at 140°C under a load of 1000 kg.

2.5 Fuel Cell Testing

The assembled MEAs were used in single cell experiments using a Fuel Cell Technologies single cell hardware and test stand. The cell had serpentine flow channels in a graphitic carbon plate with an active area of 5 cm^2. Polarization curves and potentio-electrochemical impedance spectroscopy (PEIS) were collected using a BioLogic VSP3 potentiostat and 10 A booster. A flow rate of 100 mL min^{-1} of ultra- high purity hydrogen gas (H_2) was applied at the anode and 200 mL min^{-1} of ultra- high purity oxygen gas (O_2) was applied at the cathode. All gases were at 100% relative humidity, backpressures at both electrodes were 2 atmospheres gauge (29.4 psig), and the temperature of the cell was maintained at 80°C. For testing protocol, the cell was conditioned by holding voltage at open circuit voltage (OCV) for 10 min, followed by 0.6 V for 15 min and then 0.4 V for 15 min. Polarization curves were collected by

changing the potential from OCV to 0.65 V in 2 mV increments and then from 0.65 V to 0.2 V in 20 mV increments, holding each potential for 30 seconds before recording the current.

3 Application and Discussion of Results

3.1 Physicochemical Characterization

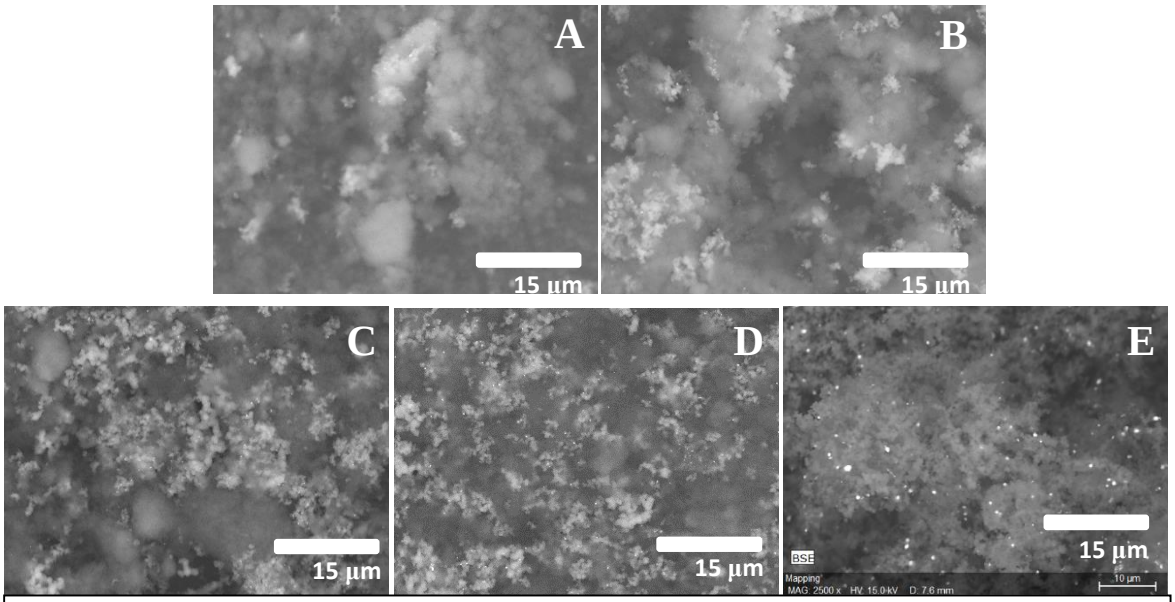

Figure 1: *Scanning electron microscopy imaging of samples. From left to right:* **(A)** 20% PCPF-Fe / 80% KJB; **(B)** 33% PCPF-Fe / 67% KJB **(C)** 43% PCPF-Fe / 57% KJB; **(D)** 50% PCPF-Fe / 50% KJB; **(E)** 100% PCPF-Fe

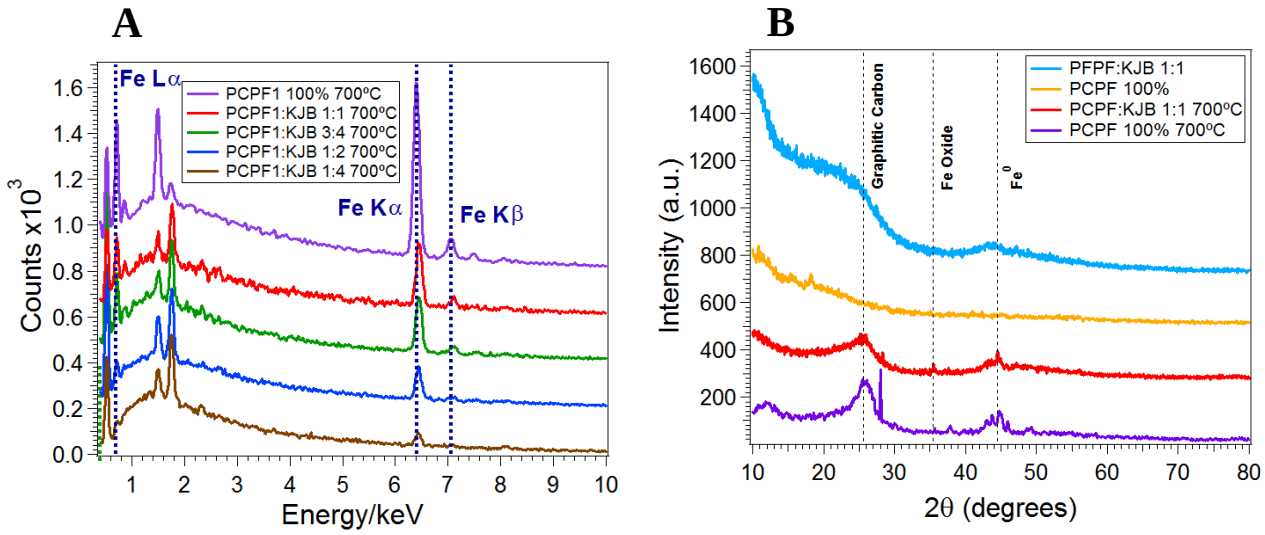

Figure 2: **(A) (left).** Energy Dispersive X-ray spectroscopy (EDS) patterns for each of the ratios of PCPF-Fe / KJB, each after a 700 °C heat treatment. **(B) (right).** X- ray diffraction patterns of both the 100% CHF-1 and 50% CHF-1 / KJB as- prepared and after a 700 °C heat treatment.

Table 1: **(A)** (**top**). Average percent weight composition of iron in the samples, prepared as listed. **(B)** (**bottom**). Average percent weight composition of PCPF-Fe in the samples, given the approximate weight percentage of iron in 100 % PCPF-Fe when prepared as listed.

	wt. % Fe		
Sample	As- Prepared	Heat Treated	Heat- Acid- Heat treated
100%	5.64	5.39	3.84
50%	2.141	1.977	0.456
43%	2.163	2.07	-
33%	1.4	1.16	-
20%	-	0.62	-

Scanning electron microscopy imaging of the PCPF-Fe catalyst samples after 700 °C heat treatments are shown in Figure 1. These images show the presence of metallic iron particles throughout the carbon structure using back-scattered electron (BSE) microscopy. Iron particles show up as relatively bright spots in the structure due to their higher atomic number. The particles appear in a homogeneous scattering throughout the sample space with few areas of high conglomeration.

EDS patterns of the samples after heat treatment are shown in figure 2(A). The plots can be used to find rough percent compositions of specific elements. Noticing that the iron peaks for the 100 % PCPF are much higher than the any of the other samples confirms a higher composition of iron, present in the porphyrin framework.

XRD scattering patterns for the 100 % and 50 % PCPF- Fe both before and after heat treatment are shown in figure 2(B). One should notice the presence of graphitic carbon and metallic iron peaks in the samples post- heat treatment, while they are absent before. A small iron oxide peak was also observed in the heat treated samples, though the inert atmosphere during pyrolysis prevented excessive iron oxidation.

Table 1(A) collects composition data from the EDS samples in figure 2(A) to find approximate weight percentages of iron in the samples. Given the weight percentages of iron in PCPF-Fe supplied by Cantillo's work (2016), table 1(B) finds approximate weight percentages of PCPF-Fe in the sample. As expected, a rough negative correlation is seen in both tables 1(A) and 1(B) between amount of carbon added to the sample and percent weight of iron or PCPF-Fe in it. However, a slight increase is observed from 50 % to 43 % PCPF-Fe / KJB, where conceptually it should decrease as the amount of carbon added has increased. One explanation for the irregularity is the low number of EDS sample sizes obtained during imaging, with some samples having only two collections to average into table 1.

3.2 Catalytic Activity: RRDE Technique

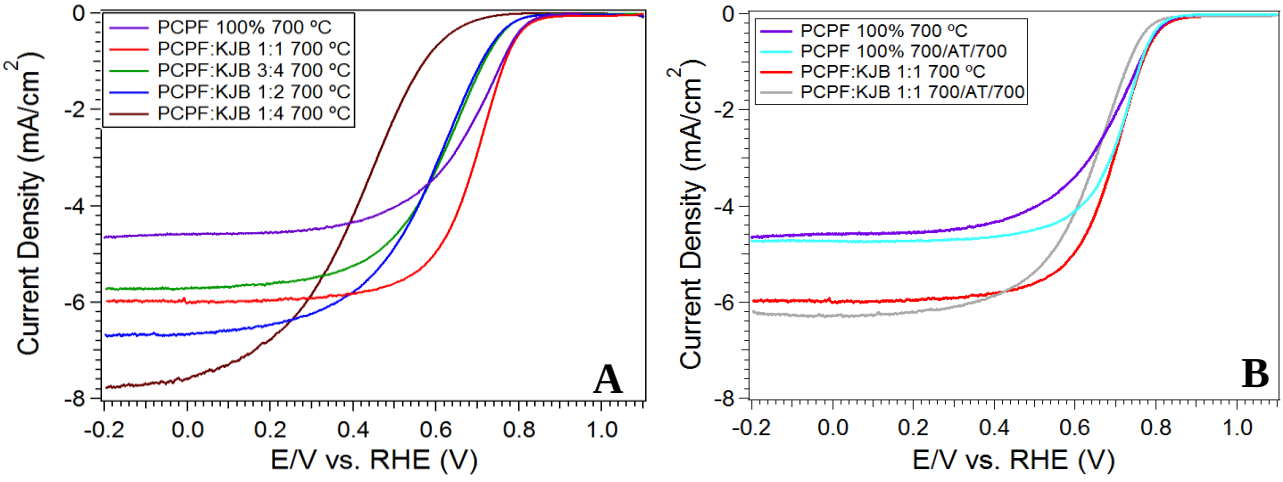

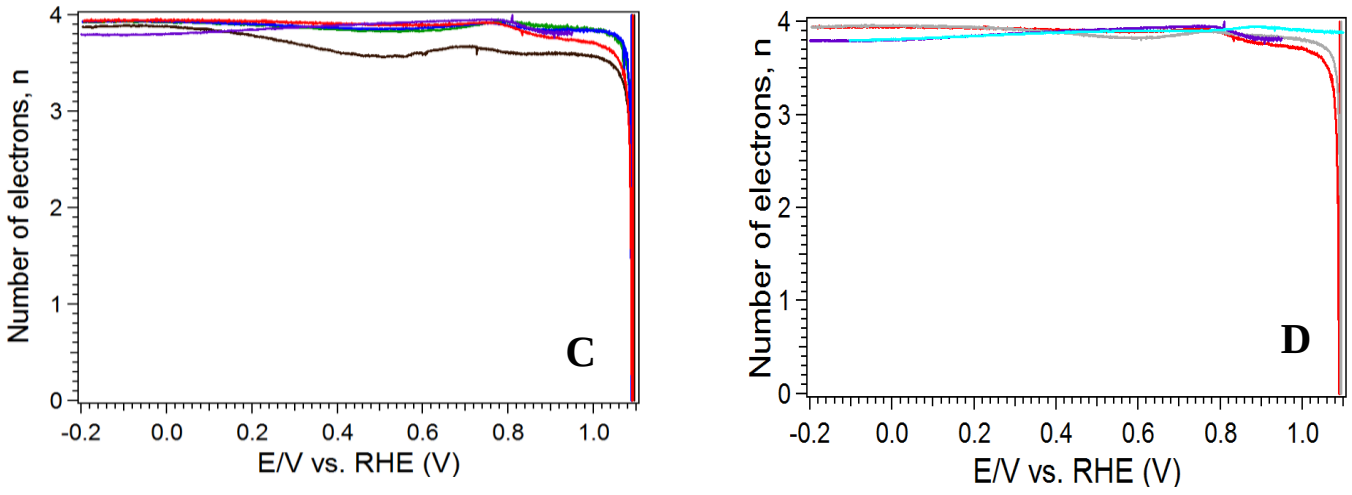

Figure 3: **(A) (top-left).** RRDE data for the various ratios of PCPF-Fe to KJB after heat treatment at 700 °C. **(B) (top-right).** RRDE data for the 100% and 50 % PCPF-FE / KJB samples after heat and acid treatment. **(C) (bottom-left).** Ring data for samples in figure 3(A), as number of electrons transferred vs potential. **(D) (bottom-right).** Ring data for samples in figure 3(B), as number of electrons transferred vs potential.

Initial rotating ring disk electrode experiment data of the PCPF-Fe samples heat treated at 700 °C is shown in figure 3(A-D). The onset potential, or the point where the potential applied to the cathode is low enough to allow a current greater than or equal to 50 $\mu A/cm^2$, appears slightly higher in the 50 % than the 100 % PCPF-Fe as shown in figure 3(A); the OCV for these samples is approximately 1.016 V and 0.868 V, respectively. As the concentration of carbon in the sample increases in the 3:4, 1:2, and 1:4 (PCPF-Fe : KJB) ratios, the the OCV appears to drop significantly, down to 0.746 V in the 1:4 sample. Although not displaying a perfectly positive trend, the limiting current density for a sample appears to increase as the amount of carbon in that sample also increases; the 1:4 PCPF-Fe : KJB shows the highest limiting current density at approximately 7.783 mA / cm^2. The number of electrons transferred in samples shown in figures 3(A) and 3(C) average between 3.8 and 3.9 below 0.8 V for all except the 1:4 sample, which transfers anywhere from 3.9 to 3.5 electrons. This suggests that for all except the aforementioned sample, the peroxide creation is only 5 to 10% of the total products.

Figure 3(B) shows the effects of acid treatment and a final heat treatment at 700 °C for the 100% and 50% (1:1 PCPF-Fe : KJB) samples. In the control 100% PCPF-Fe, the OCV appears to decrease slightly from 0.868 V in the heat treated catalyst to 0.861 V in the acid treated one. Additionally, the OCV for the 50% PCPF-Fe appears to have decreased from 1.016 V to 0.909 V after acid treatment. The change in OCV for the sample with carbon is likely due to some structure change in the catalyst due to the acid and additional heat treatment. Through the acid treatment, the nature of the active sites in a catalyst can change in terms of the coordination of the nitrogen and carbon in the structure. Various species (such as sulfate or bisulfate groups from the sulfuric acid) can also be adsorbed in the sample, affecting performance. Limiting current density changes due to acid treatment are negligible and inconclusive. Finally, the number of electrons transferred from all samples in figures 3(B) and 3(D) remains between 3.8 and 3.9 below 0.8 V.

3.3 Fuel Cell Testing

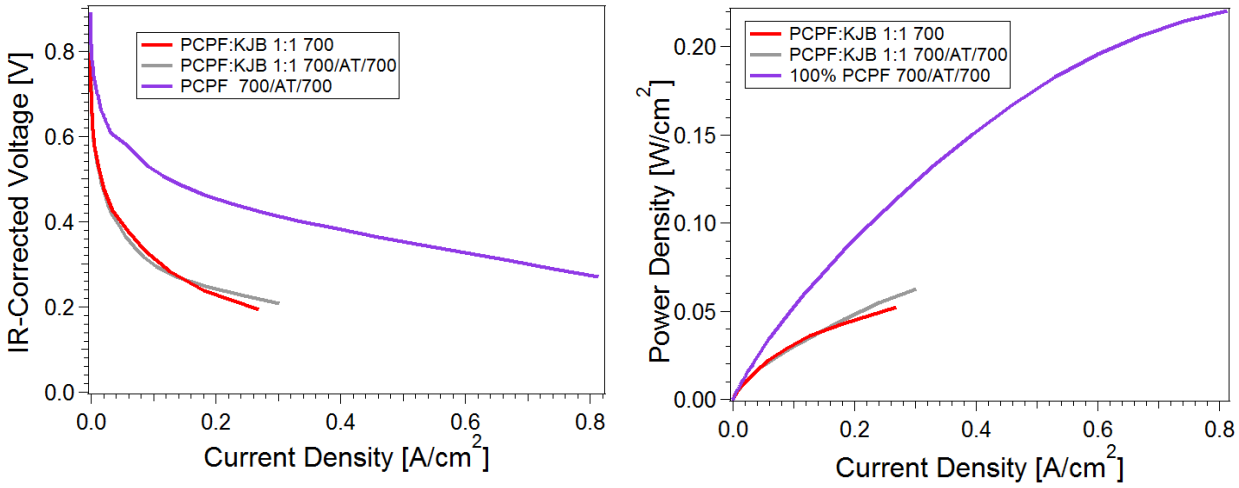

Figure 4: **(A)** (**left**). IR-corrected Voltage vs. Current Density plot for the control 100% PCPF-Fe heat treated at 700 °C, the 1:1 PCPF- Fe : KJB heat treated, and the 1:1 PCPF-Fe : KJB acid treated. **(B)** (**right**). Power density vs current density plot for the aforementioned samples

Single cell testing data for the control 100 % PFPF-Fe heat treated and the 1:1 PCPF-Fe:KJB (heat treated and heat-acid-heat treated) samples are shown in Fig. 4. Varying from what was observed in the RRDE data, the OCV for the 50% PCPF-Fe samples appears much lower than the 100 %. Additionally, the limiting current density for the 50% sample only reached approximately 0.3 A/ cm^2; acid treatment only slightly increased the limiting current density, though negligibly so compared to the control. Even under acid treatment, the limiting current density (LCD) for the 50 % PCPF-Fe was less than 40 % of the control -100 % PCPF-Fe's- LCD. Figure 4(B) shows the power density vs current density plots for each of the samples, and reveals that the limiting power density (LPD) for the 50 % PCPF-Fe, even after acid treatment, was approximately 25 % of the control's LPD.

4 Conclusion

An iron (III) porphyrin framework (PCPF-Fe) pyrolyzed with various amounts of graphitic carbon (Ketjenblack®) was analyzed as a catalyst for the ORR reaction catalyst in a Proton Exchange Membrane Fuel Cell. Although pyrolysis was found to greatly increase the catalytic activity of the material, further acid treatment was not shown to significantly improve its performance. Of the various sample ratios created, the 50% PCPF-Fe / KJB was found to have the highest onset potential, when compared to the control sample, in a rotating ring disk electrode experiment; the 50% sample also showed a limiting current density nearly 30% higher than the 100% PCPF-Fe. However, single cell testing of the sample showed severely diminished performance compared to the 100% PCPF-Fe, with limiting current density and limiting power density for the former only 40% and 25% that of the latter, respectively.

5 Acknowledgements

The authors of this paper would like to acknowledge the NSF-funded TN-SCORE program, NSF grant EPS-1004083, under Thrust 2, for supporting this set of research. I would also like to thank my research advisors, Dr. Thomas Zawodzinski Jr., Dr. Gabriel Goenaga, Dr. Shengqian Ma, and Nelly Cantillo for their instructions and advice. From Dr. Zawodzinski's "Z Group," I would like to thank the following for their assistance in various experiments: Asa Roy, Samantha Medina, and Matthew Sodl.

6. References

1. E. Proietti, F. Jaouen, M. Lefèvre, N. Larouche, J. Tian, J. Herranz, J.-P. Dodelet, 2011, Iron-based cathode catalyst with enhanced power density in polymer electrolyte membrane fuel cells, Nature Communications, pp. 1-9.

2. Frédéric Jaouen, Eric Proietti, Michel Lefèvre, Régis Chenitz, Jean-Pol Dodelet, Gang Wu, Hoon Taek Chung, Christina Marie Johnston and Piotr Zelenay, 2011, Recent advances in non-precious metal catalysis for oxygen-reduction reaction in polymer electrolyte fuel cells, Energy Environ. Sci., pp. 114-130.

3. G. Goenaga, S. Ma, S. Yuan, D.-J. Liu, 2010, New Approaches to Non-PGM Electrocatalysts Using Porous Framework Materials, The Electrochemical Society, pp. 579- 586.

4. G. Lalande, R. Cote, D. Guay, J.-P. Dodelet, L.-T. Weng, P. Bertrand, 1997, Is nitrogen important in the formulation of Fe-based catalysts for oxygen reduction in solid polymer fuel cells?, Electrocimica Acta, pp. 1379-1388.

5. G. Liu, X. Li, P. Ganesan and B. N. Popov, 2009, Development of non-precious metal oxygen-reduction catalysts for PEM fuel cells based on N-doped ordered porous carbon, Applied Catalysis B: Environmental: Elsevier, pp. 156-165.

6. G. Wu, Z. Chen, K. Artyushkova, F. H. Garzon and P. Zelenay, 2008, Polyaniline-Derived Non-Precious Catalyst For The Polymer Electrolyte Fuel Cell Cathode, ECS Trans., The Electrochemical Society, pp. 159-170.

7. Hubert A Gasteiger, Shyam S Kocha, Bhaskar Sompalli, Frederick T Wagner, 2005, Activity benchmarks and requirements for Pt, Pt-alloy, and non-Pt oxygen reduction catalysts for PEMFCs, Applied Catalysis B: Environmental: Elsevier, pp. 9-35.

8. J. Zagal, F. Bedioui and J. P. Dodelet, Eds., 2007, N4-Macrocyclic Metal Complexes, Springer-Verlag New York.

9. N. Cantillo, G. Goenaga, W. Gao, K. Williams, C. Neal, S. Ma, K. L. More, T.A. Zawodzinski, 2016, Investigation of a Microporous Iron (III) Porphyrin Framework Derived Cathode Catalyst in PEM Fuel Cells, Journal of Materials Chemistry A 2016, pp. 2-6.

10. W. Aldred, I. Bae, S. Gupta, D. Tyrk, E. Yeager, 1989, Heat-Treated Polyacrylonitrile-Based Catalysts For Oxygen Electroreduction, Journal of Applied Electrochemistry: Kluwer Academic Publishers, pp. 19-27.

11. X.-S. Wang, M. Chrzanowski, D. Yuan, B. Sweeting, S. Ma, 2014, Covalent Heme Framework as a Highly Active Heterogeneous Biomimetic Oxidation Catalyst, Chem. Mater., pp. 1639-1644

12. Zhongwei Chen, Drew Higgins, Aiping Yu, Lei Zhang, and Jiujun Zhang, 2011, A review on non-precious metal electrocatalysts for PEM fuel cells, Energy Environ. Sci., pp. 3167-3192